Organic & Biomolecular Chemistry

Intermolecular binding preferences of haloethynyl halogen-bond donors as a function of molecular electrostatic potentials in a family of N-(pyridin-2-yl)amides

Journal:	*Organic & Biomolecular Chemistry*
Manuscript ID	OB-ART-06-2021-001133.R1
Article Type:	Paper
Date Submitted by the Author:	11-Jul-2021
Complete List of Authors:	Abeysekera, Amila; Kansas State University, Chemistry Averkiev, Boris; Kansas State University, Chemistry LeMagueres, Pierre; Rigaku Americas Corporation Aakeröy, Christer; Kansas State University, Chemistry

ARTICLE

Intermolecular binding preferences of haloethynyl halogen-bond donors as a function of molecular electrostatic potentials in a family of N-(pyridin-2-yl)amides

Received 00th January 20xx,
Accepted 00th January 20xx

DOI: 10.1039/x0xx00000x

Amila M. Abeysekera,[a] Boris B. Averkiev[a] and Pierre Le Magueres,[b] and Christer B. Aakeröy*[a]

In order to explore how σ-hole potentials, as evaluated by molecular electrostatic potential (MEP) calculations, affect the ability of halogen atoms to engage in structure-directing intermolecular interactions, we synthesized four series of ethynyl halogen-substituted amide containing pyridines (activated targets); (N-(pyridin-2-yl)benzamides (Bz-act-X), N-(pyridin-2-yl)picolinamides (2act-X), N-(pyridin-2-yl)nicotinamides (3act-X) and N-(pyridin-2-yl) isonicotinamides (4act-X), where X=Cl/Br/I. The molecules are deliberately equipped with three distinctly different halogen-bond acceptor sites, π, N(pyr), and O=C, to determine binding site preferences of different halogen-bond donors. Crystallographic data for ten (out of a possible twelve) new compounds were thus analyzed and compared with data for the corresponding unactivated species. The calculated MEPs of all the halogen atoms were higher in the activated targets in comparison to the unactivated targets and was in the order of iodine ≈ chloroethynyl < bromoethynyl and iodoethynyl. This increased positive σ-hole potential led to a subsequent increase in propensity for halogen-bond formation. Two of the four chloroethynyl structures showed halogen bonding, and all three of the structurally characterized bromoethynyl species engaged in halogen bonding. The analogous unactived species showed no halogen bonds. Each chloroethynyl donor selected a π-cloud as acceptor, the bromoethynyl halogen-bond donors opted for either π or N(pyr) sites, whereas all halogen bonds involving an iodoethynyl halogen-bond donor (including both polymorphs of Bz-act-I), engaged exclusively with a N(pyr) acceptor site.

Introduction

Unlike in synthetic molecular chemistry, where covalent bond-making/bond-breaking reactions have been detailed in numerous named reactions, crystal structures (and physical properties, in particular) are not readily related to molecular structure.[1] However, by carefully examining the structural behavior and the preferred intermolecular interactions of specific functional groups, we may be able to make inferences about both crystal structure and physical properties of the bulk based upon molecular architecture alone.[2,3,4,5] Central to this effort is the need for a more advanced insight into how to control the balance between reversible and relatively weak non-covalent interactions, both in solution and in the solid state.[6,7,8] In this context,[9] it has been demonstrated that calculated molecular electrostatic potentials (MEPs) can serve as a useful tool for identifying the most likely, or the most prominent, (hydrogen/halogen/chalcogen)-bond donor and acceptor sites in crystalline solids. [10,11,12,13] The MEP at the tip of a halogen atom is referred to as a σ-hole,[14,15,16] and the magnitude of the σ- hole varies as a function of its relative polarizability; Cl<Br<I.[17,18,19] A positive value on the MEP surface indicates the position of a halogen-bond *donor*, whereas a negative value on a molecular surface points to the location of a σ-hole *acceptor*.

From a practical synthetic point of view, it is important to note that the σ-hole can be enhanced/increased by the presence of electron withdrawing atoms/functionalities such as flourine,[20] nitrogen[21,22] or nitro groups.[23] In addition, the MEP at the tip of a halogen atom also varies based on the hybridization of the associated carbon atom (sp^3<sp^2<sp).[24,25,26]

We recently explored the intermolecular binding preferences in the crystal structures of four series of closely related compounds, N-(pyridin-2-yl)benzamide (*Bz-series*), N-(pyridin-2-yl)picolinamides (*2Pyr-series*), N-(pyridin-2-yl)nicotinamides (*3Pyr-series*), N-(pyridin-2-yl)isonicotinamides (*4Pyr-series*), functionalized with un-activated halogen atoms.[27] We found that halogen bonding was only present in the structures of the iodinated compounds, *i.e*. in molecules carrying halogen atoms with the most positive σ-hole value. To expand the scope and complexity of this investigation, we deliberately increased the halogen-bond donor strength of the three halogen atoms (Cl, Br, and I) by attaching them to an *sp*-hybridized carbon atom (Figure 1). We know that this will increase the positive σ-hole potential,[26] and we hypothesize that this will lead to an increase in the occurrence of structure-directing interactions produced by the 'activated' halogen atoms.

[a] *Department of Chemistry, Kansas State University 213 CBC Building, 1212 Mid-Campus Dr North, Manhattan, KS 66506 - 0401*
[b] *Rigaku Americas Corporation 9009 New Trails Drive The Woodlands, TX 77381.*
Electronic Supplementary Information (ESI) available: Crystallographic data and details on CSD searches. See DOI: 10.1039/x0xx00000x

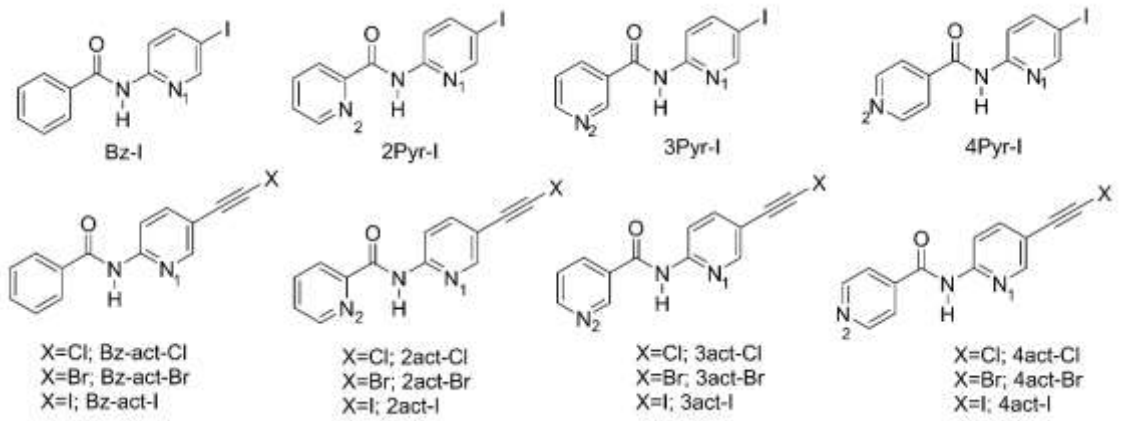

Figure 1. Target molecules in this study

Herein we will address the follwing questions;
- Will the frequency of structure-directing interactions be related to a specific/threshold σ-hole value?
- Do different haloethynyl species have a preference for certain types of acceptor sites?

Experimental

All precursors and solvents were purchased from commercial sources and used without further purification. ^{1}H and ^{13}C NMR spectra were recorded on a Bruker 400 spectrometer. Melting points were recorded on a Fisher-Johns melting point apparatus or a TA Instruments DSC Q20. Electrostatic potentials were calculated with density functional B3LYP level of theory using 6-311++G** basis set in vacuum, using Spartan 08' software.

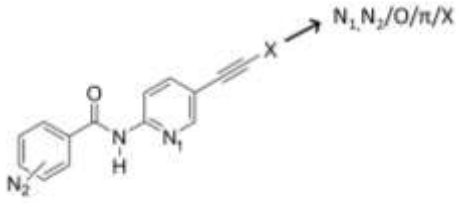

Figure 2. Postulated binding sites of the halogen bond donor

Datasets for single-crystal X-ray diffraction were collected on a Rigaku XtaLAB Synergy-S.

Synthesis

Synthesis of N-(5-((trimethylsilyl)ethynyl)pyridin-2-yl)benzamide, Bz-TMS

N-(5-iodopyridin-2-yl)benzamide/Bz-I (1.10 g, 3.30 mmol) was dissolved in 60 mL of trimethylamine: THF (1:1) and degassed with dinitrogen. CuI (0.064 g, 0.336 mmol), bis(triphenylphosphine)palladium(II) dichloride (0.216 g, 0.33 mmol) and trimethylsilylacetylene (0.72 mL, 5.00 mmol), were added and the reaction mixture was heated overnight at 80°C under dinitrogen. The reaction was monitored by TLC. The reaction medium was filtered, and the filtrate evaporated to dryness and redissolved in methylene chloride. The organic layer was washed with 1M HCl, brine, water and dried with anhydrous magnesium sulfate and filtered. The organic layer was concentrated, and the product purified by column chromatography (hexane followed by hexane: ethyl acetate 80:20). Yield 80%, m.p. 139-141°C. ^{1}H NMR (400 MHz, DMSO-d_6) δ 11.04 (s, 1H), 8.50 (dd, *J* = 2.4, 0.9 Hz, 1H), 8.24 (dd, *J* = 8.7, 0.9 Hz, 1H), 8.07 – 7.99 (m, 2H), 7.94 (dd, *J* = 8.7, 2.4 Hz, 1H), 7.66 – 7.57 (m, 1H), 7.57 – 7.48 (m, 2H), 0.26 (s, 9H). ^{13}C NMR (101 MHz, DMSO-d_6) δ 165.82, 151.45, 150.35, 140.60, 133.46, 131.79, 128.04, 127.74, 114.25, 113.57, 101.73, 96.36.

Synthesis of N-(5-((trimethylsilyl)ethynyl)pyridin-2-yl)picolinamide, 2Pyr-TMS

N-(5-bromopyridin-2-yl)picolinamide/2Pyr-Br (0.986 g, 3.545 mmol) was dissolved in 60 mL of trimethylamine: THF (1:1) and degassed with dinitrogen. CuI (0.067 g, 0.35 mmol), bis(triphenylphosphine)palladium(II) dichloride (0.247 g, 0. 0.352 mmol) and trimethylsilylacetylene (0.97 mL, 7.04 mmol), were added and the reaction mixture was heated at 80°C under dinitrogen for 3 days. The reaction was monitored by TLC. The reaction medium was filtered, and the filtrate evaporated to dryness and redissolved in methylene chloride. The organic layer was washed with 1M HCl, brine, water and dried with anhydrous magnesium sulfate and filtered. The organic layer was concentrated, and the product purified by column chromatography (hexane followed by hexane: ethyl acetate 80:20). Yield 56%, m.p. 139-141°C. ^{1}H NMR (400 MHz, DMSO-d6) δ 10.54 (s, 1H), 8.78 – 8.72 (m, 1H), 8.48 (d, J = 2.2 Hz, 1H), 8.27 (d, J = 8.5 Hz, 1H), 8.24 – 8.17 (m, 1H), 8.11 (td, J = 7.7, 1.7 Hz, 1H), 7.99 (dd, J = 8.6, 2.3 Hz, 1H), 7.73 (ddd, J = 7.6, 4.7, 1.3 Hz, 1H), 0.26 (s, 9H) 13C NMR (101 MHz, DMSO-d6) δ 161.78, 150.85, 149.71, 148.48, 147.92, 141.19, 138.27, 127.45, 122.09, 114.82, 112.30, 101.52, 96.70.

Synthesis of N-(5-((trimethylsilyl)ethynyl)pyridin-2-yl)nicotinamide, 3Pyr-TMS

N-(5-bromopyridin-2-yl)nicotinamide/3Pyr-Br (1.468 g, 5.242 mmol) was dissolved in 80 mL of trimethylamine: THF (1:1) and degassed with dinitrogen. CuI (0.100 g, 0.528 mmol), bis(triphenylphosphine)palladium(II) dichloride (0.370 g, 0.528 mmol) and trimethylsilylacetylene (1.5 mL, 10.4 mmol), were added and the reaction mixture was heated at 80°C under dinitrogen 3 days. The reaction was monitored by TLC. The reaction medium was filtered, and the filtrate evaporated to dryness and redissolved in methylene chloride. The organic layer was washed with 1M HCl, brine, water and dried with anhydrous magnesium sulfate and filtered. The organic layer was concentrated, and the product purified by column chromatography (hexane followed by hexane: ethyl acetate 80:20). Yield 50%, m.p. 188-189°C. ^{1}H NMR (400 MHz, DMSO-d_6) δ 11.31 (s, 1H), 9.14 (s, 1H), 8.78 (s, 1H), 8.54 – 8.49 (m, 1H), 8.41 (s, 1H), 8.35 (dt, *J* = 8.0, 1.9 Hz, 1H), 8.23 (dd, *J* = 8.6, 0.9 Hz, 1H), 7.96 (dd, *J* = 8.6, 2.3 Hz, 1H), 7.56 (dd, *J* = 8.0, 4.7 Hz, 1H), 0.26 (s, 9H). ^{13}C NMR (101 MHz, DMSO-d_6) δ 164.60, 152.16, 151.20, 150.42, 148.74, 140.73, 135.50, 123.13, 114.54, 113.62, 101.65, 96.54

Synthesis of N-(5-((trimethylsilyl)ethynyl)pyridin-2-yl)isonicotinamide, 4Pyr-TMS

N-(5-bromopyridin-2-yl)isonicotinamide/4Pyr-Br (2.290 g, 8.234 mmol) was dissolved in 80 mL of trimethylamine: THF (1:1) and degassed with dinitrogen. CuI (0.078 g, 0.411 mmol), bis(triphenylphosphine)palladium(II) dichloride (0.288 g, 0.411 mmol) and trimethylsilylacetylene (2.30 mL, 16.46 mmol), were added and the reaction mixture was heated at 80°C under dinitrogen 3 days. The reaction was monitored by TLC. The reaction medium was filtered, and the filtrate evaporated to dryness and redissolved in methylene chloride. The organic later was washed with 1M HCl, brine, water and dried with anhydrous magnesium sulfate and filtered. The organic layer was concentrated, and the product purified by column chromatography (hexane followed by hexane: ethyl acetate 80:20). Yield 48%, m.p. 149-151°C. ^{1}H NMR (400 MHz, DMSO-d_6) δ 11.35 (s, 1H), 8.80 – 8.74 (m, 2H), 8.52 (d, *J* = 2.3 Hz, 1H), 8.22 (d, *J* = 8.7 Hz, 1H), 7.96 (dd, *J* = 8.7, 2.4 Hz, 1H), 7.93 – 7.87 (m, 2H), 0.25 (s, 9H). ^{13}C NMR (101 MHz, DMSO-d_6) δ 165.34, 151.79, 151.25, 150.70, 141.59, 122.30, 115.57, 114.55, 102.39, 97.47

Synthesis of N-(5-(chloroethynyl)pyridin-2-yl)benzamide, Bz-act-Cl

In a round bottomed flask covered with aluminium foil, acetonitrile (50 mL) was degassed with dinitrogen. N-(5-((trimethylsilyl)ethynyl)pyridin-2-yl)benzamide (0.500 g, 1.692 mmol) and AgF (0.236 g, 1.868 mmol) were added before the introduction of N-chlorosuccinimide (0.249 g, 1.868 mmol). The mixture was connected to a nitrogen inlet and stirred for 6 days. Completion of the reaction was monitored with TLC, and the resulting suspension was filtered. The filtrate was evaporated to dryness and redissolved in 150 mL of diethylether. The organic layer was washed with water and dried with anhydrous MgSO4 and concentrated *in vacuo* to obtain the pure product. Yield 34%, m.p. 111-113°C. ^{1}H NMR (400 MHz, DMSO-d_6) δ 11.04 (s, 1H), 8.56 (s, 1H), 8.23 (d, *J* = 8.6 Hz, 1H), 8.05 – 7.96 (m, 3H), 7.61 (s, 1H), 7.52 (s, 2H). ^{13}C NMR (101 MHz, DMSO-d_6) δ 166.68, 152.42, 151.51, 141.71, 134.27, 132.63, 128.86, 128.58, 114.47, 113.91, 70.66, 67.27.

Synthesis of N-(5-(bromoethynyl)pyridin-2-yl)benzamide, Bz-act-Br

In a round bottomed flask covered with aluminium foil, acetonitrile (50 mL) was degassed with dinitrogen. N-(5-((trimethylsilyl)ethynyl)pyridin-2-yl)benzamide (0.500 g, 1.692 mmol) and AgF (0.215 g, 1.694 mmol) were added to acetonitrile and the mixture was covered with aluminium foil before the introduction of N-bromosuccinimide (0.302 g, 1.694 mmol) The mixture was connected to a dinitrogen inlet and stirred for 4 days. Completion of the reaction was monitored with TLC and the resulting suspension was filtered. The filtrate was evaporated to dryness and redissolved in 150 mL of diethylether (4:1). The organic layer was washed with water and dried with anhydrous MgSO4 and concentrated *in vacuo* to obtain the pure product. Yield 30%, m.p. 111-113°C. ^{1}H NMR (400 MHz, DMSO-d_6) δ 11.02 (s, 1H), 8.53 (dd, *J* = 2.3, 1.0 Hz, 1H), 8.22 (d, *J* = 8.7 Hz, 1H), 8.01 (dd, *J* = 8.0, 1.6 Hz, 2H), 7.97 (dd, *J* = 8.7, 2.3 Hz, 1H), 7.65 – 7.56 (m, 1H), 7.56 – 7.47 (m, 2H). ^{13}C NMR (101 MHz, DMSO) δ 166.65, 152.28, 151.42, 141.61, 134.28, 132.62, 128.86, 128.58, 114.85, 114.44, 77.32, 55.65

Synthesis of N-(5-(iodoethynyl)pyridin-2-yl)benzamide, Bz-act-I

In a round bottomed flask covered with aluminium foil, acetonitrile (80 mL) was degassed with dinitrogen. N-(5-((trimethylsilyl)ethynyl)pyridin-2-yl)benzamide (1.5 g, 5.0 mmol) and AgF (0.775 g, 6.108 mmol) were added to acetonitrile and the mixture was covered with aluminium foil before the introduction of N-iodosuccinimide (1.375g, 6.108 mmol). The mixture was connected to a dinitrogen inlet and stirred. Completion of the reaction was monitored with TLC and the resulting suspension was filtered. The filtrate was evaporated to dryness and redissolved in 250 mL of diethyl ether. The organic layer was washed with water and dried with anhydrous MgSO4 and concentrated *in vacuo.* The resultant solid was purified by passing through a ~6 cm silica plug using hexane:ethyl acetate (10:1) to obtain the pure product. Yield 29%, m.p. 156-158°C (Form 1), 162-165°C (Form 2).^{1}H NMR (400 MHz, DMSO-d_6) δ 10.99 (s, 1H), 8.48 (dd, J = 2.3, 0.9 Hz, 1H), 8.20 (dd, J = 8.7, 0.9 Hz, 1H), 8.05 – 7.97 (m, 2H), 7.91 (dd, J = 8.7, 2.4 Hz, 1H), 7.64 – 7.55 (m, 1H), 7.51 (t, J = 7.5 Hz, 2H). ^{13}C NMR (101 MHz, DMSO-d6) δ 166.60, 152.07, 151.57, 141.70, 134.30, 132.60, 128.86, 128.56, 115.97, 114.35, 89.98, 21.15.

Synthesis of N-(5-(chloroethynyl)pyridin-2-yl)picolinamide, 2act-Cl

In a round bottomed flask covered with aluminium foil, acetonitrile (50 mL) was degassed with dinitrogen. N-(5-((trimethylsilyl)ethynyl)pyridin-2-yl)picolinamide (0.500 g, 1.692 mmol) and AgF (0.429g, 3.381 mmol) were added to acetonitrile before the introduction of N-chlorosuccinimide (0.452 g, 3.381 mmol). The mixture was connected to a dinitrogen inlet and stirred for 6 days. Completion of the reaction was monitored with TLC and the resulting suspension was filtered. The filtrate was evaporated to dryness and

redissolved in 150 mL ethylacetate:diethyl ether (4:1). The organic layer was washed with water and dried with anhydrous MgSO4 and concentrated *in vacuo.* The resultant solid was purified by passing through an approx. 6 cm silica plug using hexane:ethyl acetate (10:1) to obtain the pure product. Yield 9%, m.p. 113-116°C. ^{1}H NMR (400 MHz, DMSO-d6) δ 10.56 (s, 2H), 8.76 (d, J = 4.8 Hz, 2H), 8.55 (d, J = 2.3 Hz, 2H), 8.29 (d, J = 8.7 Hz, 2H), 8.21 (d, J = 7.8 Hz, 2H), 8.16 – 8.02 (m, 4H), 7.74 (dd, J = 7.7, 4.7 Hz, 2H), 7.66 – 7.52 (m, 1H), 2.50 (d, J = 4.5 Hz, 2H). ^{13}C NMR (101 MHz, DMSO-d_6) δ 162.62, 151.98, 150.67, 149.28, 148.69, 142.29, 139.07, 128.26, 122.90, 114.48, 113.19, 70.95, 67.08.

Synthesis of N-(5-(bromoethynyl)pyridin-2-yl)picolinamide, 2act-Br

In a round bottomed flask covered with aluminium foil, acetonitrile (50 mL) was degassed with dinitrogen. N-(5-((trimethylsilyl)ethynyl)pyridin-2-yl)picolinamide (0.500 g, 1.692 mmol) and AgF (0.429g, 3.381 mmol) were added to acetonitrile before the introduction of N-bromosuccinimide (0.602 g, 3.381 mmol). The mixture was connected to a dinitrogen inlet and stirred for 4 days. Completion of the reaction was monitored with TLC and the resulting suspension was filtered. The filtrate was evaporated to dryness and redissolved in 150 mL ethylacetate:diethyl ether (4:1). The organic layer was washed with water and dried with anhydrous MgSO4 and concentrated in vacuo. The resultant solid was purified by passing through an approx. 6 cm silica plug using hexane:ethyl acetate (10:1) to obtain the pure product. Yield 5%, m.p. 130 – 132 °C. ^{1}H NMR (400 MHz, DMSO-d$_6$) δ 10.55 (s, 1H), 8.77 (s, 1H), 8.52 (s, 1H), 8.28 (d, J = 8.6 Hz, 1H), 8.21 (d, J = 7.8 Hz, 1H), 8.12 (s, 1H), 8.04 (d, J = 8.6 Hz, 1H), 7.74 (s, 1H). 13C NMR (101 MHz, DMSO-d6) δ 162.58, 151.86, 150.53, 149.33, 149.27, 148.69, 142.19, 139.14, 139.07, 128.25, 122.90, 115.40, 113.15, 77.12, 56.01.

Synthesis of N-(5-(iodoethynyl)pyridin-2-yl)picolinamide, 2act-I

In a round bottomed flask covered with aluminium foil, acetonitrile (50 mL) was degassed with dinitrogen. N-(5-((trimethylsilyl)ethynyl)pyridin-2-yl)picolinamide (0.500 g, 1.692 mmol) and AgF (0.253 g, 1.994 mmol) were added to acetonitrile before the introduction of N-iodosuccinimide (0.458 g, 2.035 mmol). The mixture was connected to a dinitrogen inlet and stirred overnight. Completion of the reaction was monitored with TLC and the resulting suspension was filtered. The filtrate was evaporated to dryness and redissolved in 150 mL ethylacetate:diethyl ether (4:1). The organic layer was washed with water and dried with anhydrous MgSO4 and concentrated *in vacuo.* The resultant solid was purified by passing through an approx. 6 cm silica plug using hexane:ethyl acetate (10:1) to obtain the pure product. Yield 5%. m.p. 165 – 167°C. ^{1}H NMR (400 MHz, DMSO-d_6) δ 10.52 (s, 1H), 8.76 (s, 1H), 8.47 (s, 1H), 8.24 (d, *J* = 20.6 Hz, 2H), 8.12 (s, 1H), 7.98 (s, 1H), 7.74 (s, 1H). ^{13}C NMR (101 MHz, DMSO-d_6) δ 162.55, 152.05, 150.33, 149.28, 148.72, 142.29, 139.06, 128.24, 122.89, 116.51, 113.06, 89.79, 21.64.

Synthesis of N-(5-(chloroethynyl)pyridin-2-yl)nicotinamide, 3act-Cl

In a round bottomed flask covered with aluminium foil, acetonitrile (50 mL) was degassed with dinitrogen. N-(5-((trimethylsilyl)ethynyl)pyridin-2-yl)nicotinamide (1.00 g, 3.38 mmol) and AgF (0.858 g, 6.7 mmol) were added to acetonitrile before the introduction of N-chlorosuccinimide (0.994 g, 6.7 mmol). The mixture was connected to a dinitrogen inlet and stirred for 7 days. Completion of the reaction was monitored with TLC and the resulting suspension was filtered. The filtrate was evaporated to dryness and redissolved in 150 mL ethylacetate:diethyl ether (4:1). The organic layer was washed with water and dried with anhydrous MgSO4 and concentrated *in vacuo.* The resultant solid was purified by passing through an approx. 6 cm silica plug using hexane:ethyl acetate (10:1) to obtain the pure product. Yield 8.5%, decomp. 199 – 201°C. ^{1}H NMR (400 MHz, DMSO-d_6) δ 11.31 (s, 1H), 9.12 (s, 1H), 8.77 (s, 1H), 8.57 (s, 1H), 8.33 (s, 1H), 8.22 (s, 1H), 8.00 (s, 1H), 7.55 (s, 1H). 13C NMR (101 MHz, CDCl3) δ 167.60, 155.35, 154.52, 153.92, 151.92, 146.77, 144.21, 138.70, 132.51, 126.28, 116.87, 73.18, 69.56

Synthesis of N-(5-(bromoethynyl)pyridin-2-yl)nicotinamide, 3act-Br

In a round-bottomed flask covered with aluminium foil, acetonitrile (50 mL) was degassed with dinitrogen. N-(5-((trimethylsilyl)ethynyl)pyridin-2-yl)nicotinamide (0.500 g, 1.692 mmol) and AgF (0.429g, 3.381 mmol) were added to acetonitrile before the introduction of N-bromosuccinimide (0.602 g, 3.381 mmol). The mixture was connected to a dinitrogen inlet and stirred for 7 days. Completion of the reaction was monitored with TLC and the resulting suspension was filtered. The filtrate was evaporated to dryness and redissolved in 150 mL ethylacetate:diethyl ether (4:1). The organic layer was washed with water and dried with anhydrous MgSO4 and concentrated *in vacuo.* The resultant solid was purified by passing through an approx. 6 cm silica plug using hexane:ethyl acetate (10:1) to obtain the pure product. Yield 4% ^{1}H NMR (400 MHz, DMSO-d_6) δ 11.30 (s, 1H), 9.12 (s, 1H), 8.77 (s, 1H), 8.54 (s, 1H), 8.34 (s, 1H), 8.21 (s, 1H), 8.00 (s, 1H), 7.53 (s, 1H). ^{13}C NMR (101 MHz, DMSO-d_6) δ 165.43, 152.99, 152.03, 151.49, 149.56, 141.75, 136.35, 130.17, 123.91, 115.15, 114.48, 55.85, 49.07

Synthesis of N-(5-(iodoethynyl)pyridin-2-yl)nicotinamide, 3act-I

In a round bottomed flask covered with aluminium foil, acetonitrile (50 mL) was degassed with dinitrogen. N-(5-((trimethylsilyl)ethynyl)pyridin-2-yl)nicotinamide (0.500 g, 1.692 mmol) and AgF (0.215 g, 1.692 mmol) were added to acetonitrile before the introduction of N-iodosuccinimide (0.380 g, 1.692 mmol). The mixture was connected to a dinitrogen inlet and stirred for 7 days. Completion of the reaction was monitored with TLC and the resulting suspension was filtered. The filtrate was evaporated to dryness and redissolved in 150 mL ethylacetate:diethyl ether (4:1). The organic layer was washed with water and dried with anhydrous

MgSO4 and concentrated *in vacuo.* The resultant solid was purified by passing through an approx. 6 cm silica plug using hexane:ethyl acetate (10:1) to obtain the pure product. Yield 10%, decomp. 192-194°C. ^{1}H NMR (400 MHz, DMSO-d_6) δ 11.27 (s, 1H), 9.12 (s, 1H), 8.76 (d, *J* = 4.9 Hz, 1H), 8.50 (d, *J* = 2.2 Hz, 1H), 8.33 (dt, *J* = 8.1, 1.9 Hz, 1H), 8.20 (d, *J* = 8.6 Hz, 1H), 7.93 (dd, *J* = 8.7, 2.3 Hz, 1H), 7.55 (dd, *J* = 8.0, 4.8 Hz, 1H). ^{13}C NMR (101 MHz, DMSO-d_6) δ 165.37, 152.95, 151.81, 151.63, 149.54, 141.83, 136.33, 130.19, 123.90, 116.25, 114.39, 89.92, 21.39.

Synthesis of N-(5-(chloroethynyl)pyridin-2-yl)isonicotinamide, 4act-Cl

In a round-bottomed flask covered with aluminium foil, acetonitrile (80 mL) was degassed with dinitrogen. N-(5-((trimethylsilyl)ethynyl)pyridin-2-yl)isonicotinamide (1.000 g, 3.385 mmol) and AgF (1.06 g, 8.47 mmol) were added to cetonitrile before the introduction of N-chlorosuccinimide (1.127 g, 8.444 mmol). The mixture was connected to a dinitrogen inlet and stirred for 7 days. Completion of the reaction was monitored with TLC and the resulting suspension was filtered. The filtrate was evaporated to dryness and redissolved in 150 mL ethylacetate:diethyl ether (4:1). The organic layer was washed with water and dried with anhydrous MgSO4 and concentrated *in vacuo.* The resultant solid was purified by passing through an approx. 6 cm silica plug using hexane:ethyl acetate (10:1) to obtain the pure product. Yield 6.5%, decomp. 184-186°C. ^{1}H NMR (400 MHz, DMSO-d_6) δ 11.36 (s, 1H), 8.81 – 8.75 (m, 2H), 8.58 (dd, *J* = 2.3, 0.9 Hz, 1H), 8.23 (dd, *J* = 8.7, 0.9 Hz, 1H), 8.03 (dd, *J* = 8.7, 2.3 Hz, 1H), 7.93 – 7.87 (m, 2H), 1.23 (s, 1H). ^{13}C NMR (101 MHz, DMSO-d_6) δ 165.38, 151.93, 151.59, 150.70, 141.90, 141.42, 122.31, 114.63, 114.43, 70.88, 67.15.

Synthesis of N-(5-(bromoethynyl)pyridin-2-yl)isonicotinamide, 4act-Br

In a round bottomed flask covered with aluminium foil, acetonitrile (80 mL) was degassed with dinitrogen. N-(5-((trimethylsilyl)ethynyl)pyridin-2-yl)isonicotinamide (0.980 g, 3.317 mmol) and AgF (1.180 g, 6.628 mmol) were added to acetonitrile before the introduction of N-bromosuccinimide (0.840 g, 6.628 mmol). The mixture was connected to a dinitrogen inlet and stirred for 6 days. Completion of the reaction was monitored with TLC and the resulting suspension was filtered. The filtrate was evaporated to dryness and redissolved in 150 mL ethylacetate:diethyl ether (4:1). The organic layer was washed with water and dried with anhydrous MgSO4 and concentrated *in vacuo.* The resultant solid was purified by passing through an approx. 6 cm silica plug using hexane:ethyl acetate (10:1) to obtain the pure product. Yield 10%, m.p. 179-181°C. ^{1}H NMR (400 MHz, DMSO-d_6) δ 11.34 (s, 1H), 8.76 (s, 2H), 8.56 (s, 1H), 8.22 (s, 1H), 8.01 (s, 1H), 7.89 (s, 2H).

Synthesis of N-(5-(iodoethynyl)pyridin-2-yl)isonicotinamide, 4act-I

In a round bottomed flask covered with aluminium foil, acetonitrile (50 mL) was degassed with dinitrogen. N-(5-((trimethylsilyl)ethynyl)pyridin-2-yl)isonicotinamide (0.800 g, 2.708 mmol) and AgF (0.375 g, 2.955 mmol) were added to acetonitrile before the introduction of N-iodosuccinimide (0.667 g, 2.964 mmol). The mixture was connected to a dinitrogen inlet and stirred for 3 days. Completion of the reaction was monitored with TLC and the resulting suspension was filtered. The filtrate was evaporated to dryness and redissolved in 150 mL ethylacetate:diethyl ether (4:1). The organic layer was washed with water and dried with anhydrous MgSO4 and concentrated *in vacuo*. The resultant solid was purified by passing through an approx. 6 cm silica plug using hexane:ethyl acetate (10:1) to obtain the pure product. Yield 8%, decomp. 215-217°C. 1H NMR (400 MHz, DMSO-d6) δ 11.32 (s, 1H), 8.77 (s, 2H), 8.50 (s, 1H), 8.19 (s, 1H), 7.95 (s, 1H), 7.89 (s, 2H). 13C NMR (101 MHz, DMSO-d6) δ 165.29, 151.65, 151.57, 150.66, 141.88, 141.49, 122.32, 116.47, 114.52, 89.88, 21.59.

Results

Molecular electrostatic potentials, MEPs

The calculated MEP values for all molecules targeted in this study are shown in Figure 3.

Single-crystal X-ray diffraction, SCXRD

The crystal structures for the four unactivated targets have been previously reported.[27] Of the 12 new activated compounds prepated, crystallographic data were obtained for ten of them, as well as two polymorphs of **Bz-act-I**. The solvents used for crystal growth are listed in Table.1.

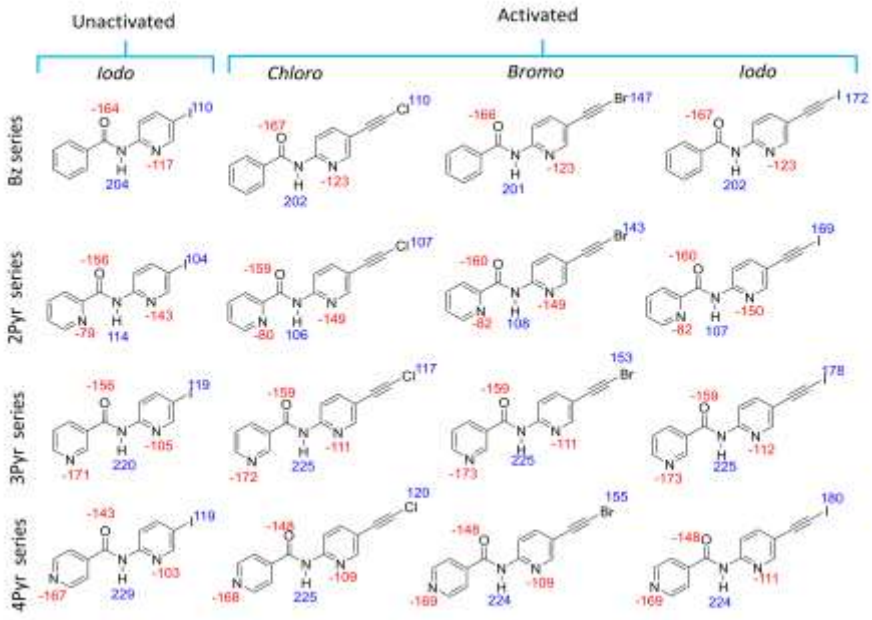

Figure 3. MEP values at most likely acceptor and donor sites (kJ/mol).

Table 1 Solvents used for crystal growth and crystal descriptions

Compound	Code	Solvent	Color and morphology
N-(5-(chloroethynyl)pyridin-2-yl)benzamide	Bz-act-Cl	Methanol	Colorless, plate
N-(5-(bromoethynyl)pyridin-2-yl)benzamide	Bz-act-Br	Methanol	Light yellow, plate
N-(5-(iodoethynyl)pyridin-2-yl)benzamide	Bz-act-I (Form 1)	Methanol	Yellow, block
	Bz-act-I (Form 2)*	Methanol	Yellow, needle
N-(5-(chloroethynyl)pyridin-2-yl)picolinamide	2act-Cl	Acetone	Colorless, plate
N-(5-(bromoethynyl)pyridin-2-yl)picolinamide	2act-Br	Acetone	Colorless, needle
N-(5-(chloroethynyl)pyridin-2-yl)nicotinamide	3act-Cl	Acetonitrile:Ethyl acetate	Light yellow, needle
N-(5-(iodoethynyl)pyridin-2-yl)nicotinamide	3act-I	Methanol	Yellow, block
N-(5-(chloroethynyl)pyridin-2-yl)isonicotinamide	4act-Cl	Ethyl acetate	Colorless, plate
N-(5-(bromoethynyl)pyridin-2-yl)isonicotinamide	4act-Br	Ethyl acetate	Colorless, needle
N-(5-(iodoethynyl)pyridin-2-yl)isonicotinamide	4act-I	Acetone:THF	Yellow, block

* Obtained from a failed co-crystallization experiment between **Bz-act-I** and 4-cyanobenzoic acid.

In the Bz series (Figure 4), the primary intermolecular interactions in the structure of the unactivated **Bz-I**,[27] were a N-H···N_1(py)/N_1(py)···H-N synthon, and a C-I···π halogen bond (Figure 4a). **Bz-act-Cl** and **Bz-act-Br** contain similar N-H···N(py)/N(py)···H-N synthons accompanied by C-X···π halogen bonds. Both polymorphs of **Bz-act-I** display a C-I···N_1 halogen bond. In **Bz-act-I** (Form 1), surprisingly no hydrogen bonding is shown by the amide nitrogen, while in Form 2, an N-H···O=C interaction is present, linking adjacent molecules. The relevant hydrogen- and halogen and bond geometries in the crystal structures of these compounds are given in Table 2.

Table 2: Hydrogen- and halogen bond parameters in the Bz-act compounds

Code	D-H/I···A	D/I···A (A)	D-H···A (deg)
Bz-act-Cl	N10-H10···N2	3.204(6)	168.1(1)
	C8-Cl9···C17	3.346(1)	157.4(5)
Bz-act-Br	N10-H10···N2	3.208(2)	167(2)
	C8-Br9···C17	3.336 (2)	173.60(7)
Bz-act-I (Form 1)	C8-Cl9···N2	2.884(4)	167.4(2)
Bz-act-I (Form 2)	N10-H10···O12	3.693(2)	150.51(1)
	C8-Cl9···N2	2.886(1)	169.7(7)

In the unactivated iodo compounds of the 2Pyr series, a N-H···N_2(py) intramolecular interaction and C-I···N and C-I···I halogen bonds were present (Figure 5).[27] As expected, in **2act-Cl** and **2act-Br**, the N-H···N_2(py) intramolecular hydrogen bond

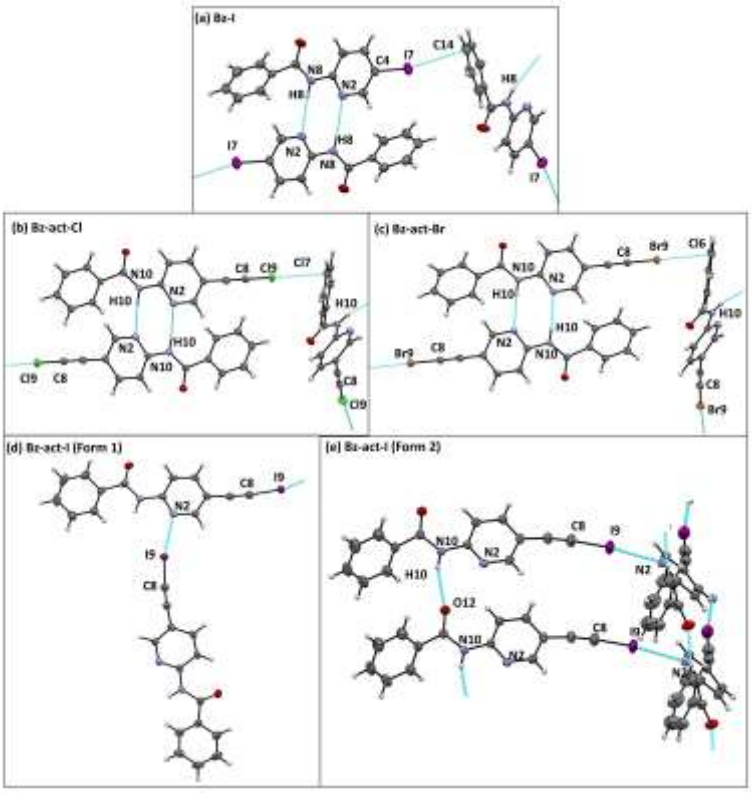

Figure 4 Primary interactions in crystal structures of (a) **Bz-I**,PACLOY [27](b) **Bz-act-Cl**, (c) **Bz-act-Br**, (d**) Bz-act-I**-(Form I), (e) **Bz-act-I-I** (Form 2)

is preserved. In **2act-Cl** an additional C-Cl···π halogen bond is present while in **2act-Br**, a C-Br···N is observed, thus, these compounds are not isostructural. The relevant hydrogen- and halogen and bond geometries are found in Table 3.

Table 3. Hydrogen- and halogen bond parameters in the 2act compounds

Code	D-H/I···A	D/I···A (A)	D-H···A (deg)
2act-Cl	N10-H10···N14	2.702(4)	110.47(1)
	C8-Cl9···C15	3.347(6)	167.14(2)
2act-Br	N10-H10···N14	2.689(1)	110.51(4)
	C8-Cl9···N2	2.940(1)	175.70(1)

In the 3Pyr series (Figure 6), the primary non-covalent interaction in the unactivated iodo compound[27]is a N-H···N_2(py) synthon and, surprisingly, no halogen bonds were present. The same is true for **3act-Cl** which contains a N-H···N_2(py) synthon with no halogen bonds present. In **3act-I**, N-H···N_1(py)/N_1(py)···H-N hydrogen bonds lead to dimer formation. Additionally, a C-I···N_2 halogen bond is formed. The relevant hydrogen- and halogen and bond geometries in these structures are given in Table 4.

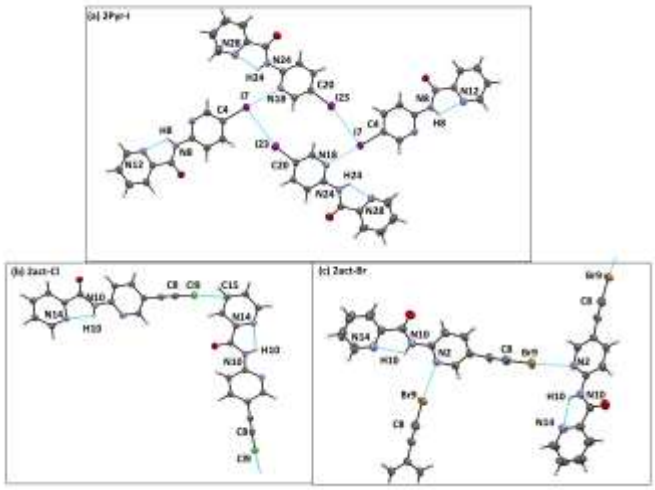

Figure 5. Primary interactions in crystal structures of (a) **2Pyr-I**, PACMIT [27](b) **2act-Cl,** (c)**2act-Br**

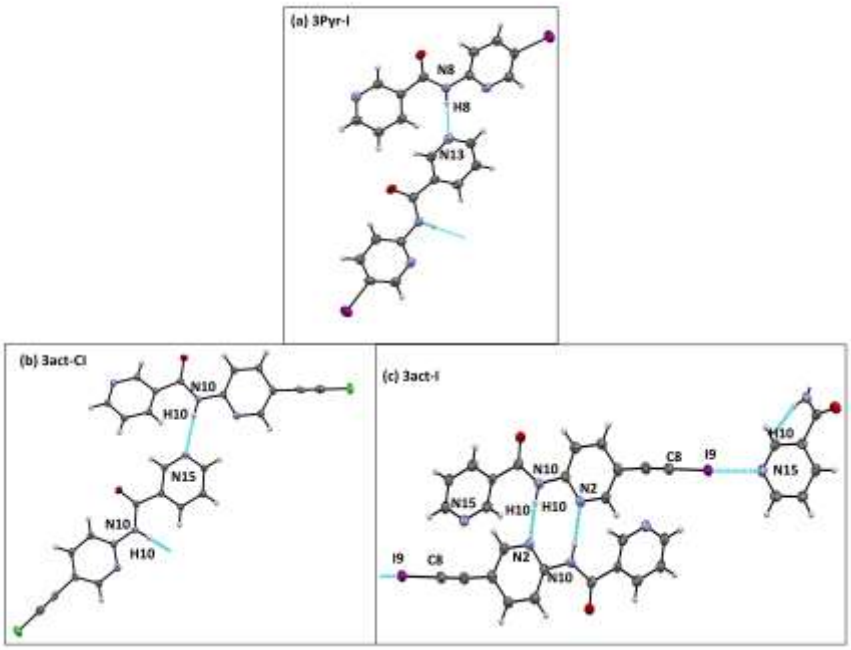

Figure 6. Primary interactions in crystal structures of (a) **3Pyr-I**,PACNEQ[27] (b) **3act-Cl** and (c) **3act-I**

Table 4 Hydrogen- and halogen bond parameters in the 3act compounds

Code	D-H/I···A	D/I···A (A)	D-H···A (deg)
3act-Cl	N10-H10···N15	3.027(2)	164.04(1)
3act-I	N10-H10···N2	3.156(5)	155.3(3)
	C8-Cl9···N15	2.793(4)	178.27(8)

In the 4Pyr targets, the unactivated iodo parent was the only compound where a halogen bond was able to compete with a hydrogen bond.[27] Two polymorphs of **4Pyr-I** (Form 1 and Form 2) were obtained[27] (Figure 7a and b). In both structures, a C-I···N_2(pyr) halogen bond was formed, accompanied by either N-H···N_1(py)/N_1(py)···H-N or N-H···O=C, respectively. In the structure of **4act-Cl**, an N-H···N_2(py) hydrogen bond leads to infinite 1-D supramolecular chains. There are no notable halogen bonds. In **4act-Br**, symmetry related dimers are produced by the H···N_1(py)/N_1(py)···H-N synthon. Additionally, halogen bonding, C-Br···N_2(pyr) is also present. In **4act-I**, once again the H···N_1(py)/N_1(py)···H-N synthon, resulted in dimer and a C-I···N_2(pyr) halogen bond was noted (Figure 6-d). The relevant hydrogen- and halogen and bond geometries in these structures are given in Table 5.

Table 5 Hydrogen- and halogen bond parameters in the 4act compounds

Code	D-H/I···A	D/I···A (A)	D-H···A (deg)
4act-Cl	N7-H7···N16	3.150(2)	167.25(1)
4act-Br	N10-H10···N2	3.099(2)	159.77(1)
	C8-Br9···N16	2.957(2)	172.06(8)
4act-I	N10-H10···N2	3.0346(5)	138.65(8)
	C8-Cl9···N16	2.787(5)	179.86(7)

A summary of the halogen bonds in the parent iodo compounds and the activated halogen analogues is given in Table 6.

Table 6 Summary of halogen bond interactions

	Unact-I[27]	Act-Cl	Act-Br	Act-I
Bz	C-X···π	C-X···π	C-X···π	C-X···N (Form I) C-X···N (Form 2)
2Pyr	C-X···N and C-X···X	C-X···π	C-X···N	No SXCRD data
3Pyr	none	none	No SXCRD data	C-X···N
4Pyr	C-X···N (Form I) C-X···N (Form 2)	none	C-X···N	C-X···N

Discussion

Within each series, the MEPs at the acceptor sites (N, O) and amide hydrogen atom of the unactivated targets are very close to each other (within ≤ 2 kJ) regardless of the nature of the halogen atom (chloro, bromo, or iodo).[27] Within each series, the MEPs of the acceptor sites (N, O) and amide hydrogen atoms in the activated targets, are also comparable to those in the unactivated parents (within ≤ 10 kJ), Figure 8. The MEP values of halogen bond donor site within each series follow the following trend: iodo ≈ chloroethynyl < bromoethynyl < iodoethynyl. The relatively higher (more positive) MEP of N_1 and relatively lower (more negative) MEP of N_2 in 2Pyr series compared to 3Pyr and 4Pyr series may be attributed to a degree of "resonance" in the intramolecular hydrogen bonding present in the 2Pyr series targets.[27,28,29]

In the unactivated compounds, only iodine participated in a halogen bond while chlorine and bromine did not engage in any

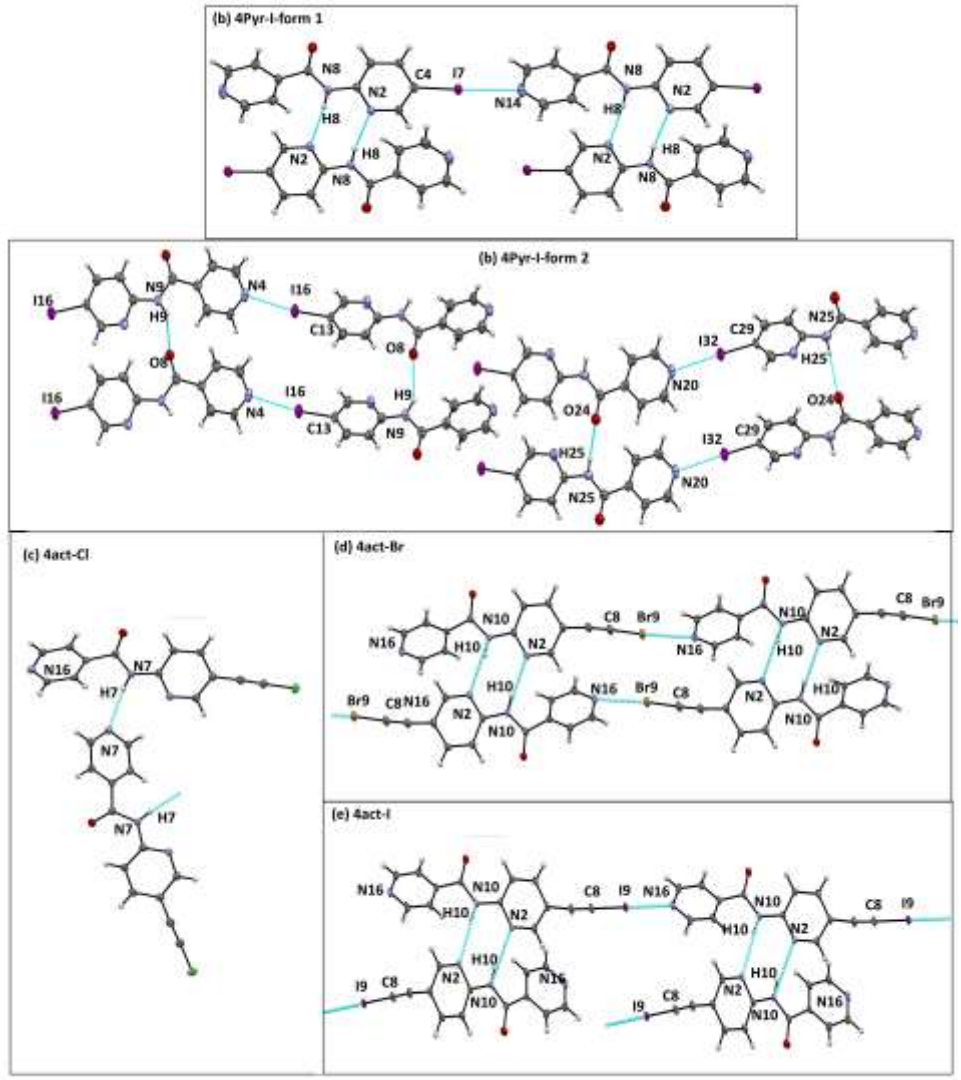

Figure 7. Primary interactions in crystal structures of (a) **4Pyr-I**(form I)PACPAO [27](b) **4Pyr-I**(form 2)PACPAO01 (c) **4act-Cl** (d) **4act-Br** (e) **4act-I**

notable short intermolecular contacts.[27] This can be readily explained by the relative differences in the MEP value of the halogen-bond donors (the iodine having the highest positive potential). When changing the carbon atom associated with the halogen atoms from an sp^2-hybridized carbon, to an *sp*-carbon, the MEP potentials of all the halogen atoms increased substantially. This covalent change effectively brought the σ-hole value of the least polarizable halogen atom (chlorine) into close proximity of that displayed by the unactivated iodine atom. The structural analysis shows that this enhancement subsequently increases the ability of the halogen atom to engage in structure directing interactions. With this deliberate activation (attachment to an ethynyl group), both chlorine and bromine began to participate in notable intermolecular interactions. In 2/4 cases (**Bz-act-Cl** and **2act-Cl**) halogen bonding was observed with chloroethynyl, and in 3/3 cases (**Bz-act-Br**, **2act-Br**, and **4act-Br**) halogen bonding was observed with bromoethynyl. The iodoethynyl compounds displayed

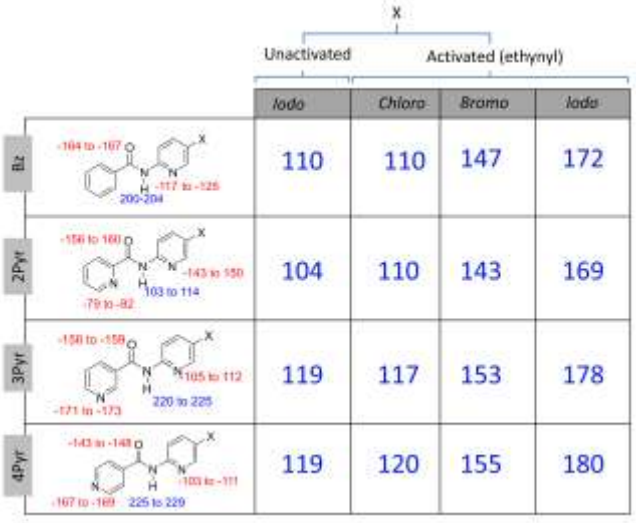

Figure 8. Summarized MEP data of compounds.

halogen bonding in all four cases. The frequency of halogen bond formation ranks in the order of chloroethynyl < iodine < bromoethynyl = iodoethynyl. Among the unactivated iodinated targets **3Pyr-I** was the only member that did not show any halogen bonding. The obstacles faced by the halogen bond donors of the series were however overcome by the iodoethynyl in **3act-I** as it displayed halogen bonding. Thus, the frequency of structure directing interactions is increased with reaching a MEP value of ≈110 kJ/mol. Of the 11 new crystal structures reported in this study, halogen bonding occurred to either π (3/11) or $N_{(pyr)}$ (6/11) while no halogen bonding occurred in 2/11 structures.

The relevant halogen-bond donors in each of the scenarios are shown (Figure 9). The chloroethynyl selected π as the acceptor, bromoethynyl selected either π or $N_{(pyr)}$ and iodoethynyl always selected $N_{(pyr)}$.

The % change in van der Waals radii of the halogen bonds of

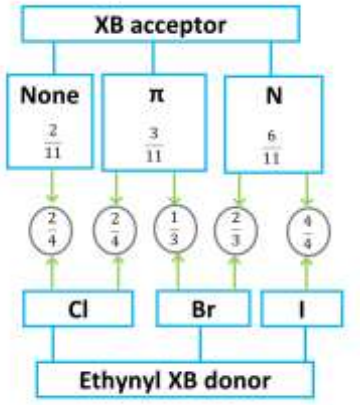

Figure 9. Summary of selected acceptor site by ethynyl XB donors

previously reported unactivated parent (iodo)[27] targets and the nine crystal structures exhibiting XB interactions in this study (total 13 structures) were investigated, Figure 10. The reduction in the combined van der Waals radii of the interaction atoms, with a π cloud (carbon atom) as the acceptor was <6%. When a pyridyl nitrogen was the acceptor, the % reduction with XB bond formation ranged from 13-20%, and changed in the order of **iodo≅bromoethynyl<iodoethynyl.**

A CSD search was carried out to compare the binding preferences of activated halogen-bond donors in reported organic, single-component crystal structures. The number of hits of ethynyl chloro, bromo and iodo compunds were 10, 22 and 74 (see supplementary data for a list of refcodes), respectively and the frequency of halogen bond formation varied in the order of 70%, 86% and 100%. When the results obtained from our current study are added to existing literature data, the combined frequency of XB fomation by ethynylchloro, ethynyl bromo and iodoethynyl varies in the order of 64%, 88% and 100%. Thus, the results obtained in this study are in good agreement with the existing trends in halogen bonding of haloethynyl compounds.

The binding sites occupied by the haloethynyl halogen-bond donors in structures reported in the CSD were also analyzed and classified as shown in Table 7.

Table 7 Acceptor site occupancy of haloethynyl XB donors reported in CSD

		Acceptor site				
		Oxygen	Nitrogen	π	Other	None
Ethynyl XB donor	Chloro	40%	10%	20%	0%	30%
		4/10	1/10	2/10	0/11	3/11
	Bromo	43%	5%	38%	0%	14%
		9/21	1/21	8/21	0/21	3/21
	Iodo	55%	16%	20%	8%	0%
		41/74	12/74	15/74	6/74	0/74

Unfortunately, none of these molecules from the CSD were equipped with both oxygen and nitrogen as possible binding sites, and therefore, a reliable assessment of preferred binding sites cannot be made. However, in our study since we deliberately selected molecules which offer the simultanoues presence of multiple binding sites (O/N/π), the results obtained serve as an ideal starting point for evaluating binding preferences of different ethynyl halogen bond donors. In this work ethynyliodo to pyridyl nitrogen occurs as a very reliable motif. This finding is consistent with recent work[30] where $N_{(pyr)}$ occurred as the most frequently occupied acceptor site by halogen-bond donors activated by a fluorine backbone. Since ethynylchloro interacted with only π, and ethnyl bromo interacted with either π or $N_{(pyr)}$, (and even though we only have a relatively small number of data points) this study illustrates that a particular preference for an acceptor site is indicated. It seems that chloroethynyl seeks out acceptors of low electron

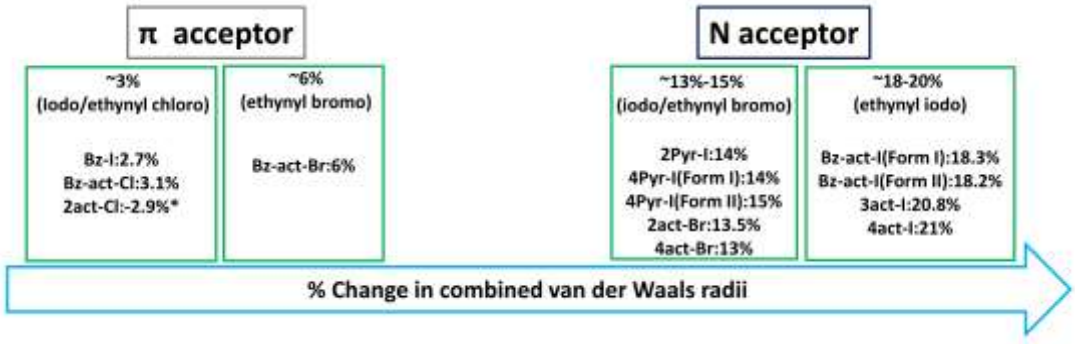

Figure 10. Reduction in the sum of the van der Waals radii of both interacting atoms, expressed in percentage points.*Although the change does not result in a reduction of bond length the XB bond is close to linear and directed towards a π cloud.

densities such as π, ethynyl bromo engage with both π or $N_{(pyr)}$, sites and iodoethynyl donors prefer to engage with $N_{(pyr)}$.

Conclusions

In previously reported work on N-(pyridinyl)benzamides, N-(pyridinyl)picolinamides, N-(pyridinyl)nicotinamides and N-(pyridinyl)isonicotinamides substituted with unactivated halogen atoms[27], no structure directing interactions were shown by either chlorine (0/4) or bromine (0/4) while iodine did (4/5). Here, we increased the MEP of all three halogens by connecting them to an *sp*-hybridized carbon atom.

Upon activation, the σ-hole values rank in the order of chloroethynyl ≈ iodine < bromoethynyl < iodoethynyl. Even though the unactivated iodine and chloroethynyl targets had comparable σ-hole values, the frequency of XB formation as well as the choice of acceptor sites were different for these two XB donors. Thus, the halogen-bond forming frequency varies in the order of chloroethynyl < iodine < bromoethynyl = iodoethynyl. Chloroethynyl and iodine formed halogen bonds with π or $N_{(pyr)}$, whereas the iodoethynyl halogen-bond donor consistently engaged in halogen bonds with the pyridyl nitrogen atom acceptor site.

It should also be noted that the overall stability and strength of a halogen bond is determined by contributions from electrostatic,[31] charge-transfer[32] dispersion and polarization[33] components, and the relative importance of each, is still under debate.[34] Establishing correlations between molecular electrostatic potentials (MEPs) mapped onto molecular surfaces and experimentally determined crystal structures, is integral to the development of concepts such as σ-hole and π-hole, both of which are very useful for identifying intermolecular interactions between closed shell systems. Despite the simplicity of this electrostatic view of halogen bonding, MEPS can provide considerable insight into how molecules recognize, bind and aggregate into extended solid-state architectures. In this study we hope to have demonstrated that calculated MEPs can provide simple descriptions of the structural consequences involving supramolecular synthons that can be of practical benefits to crystal engineering.

Supplementary information

Deposition Number(s) 2089318 (Bz-act-Cl), 2089319 (Bz-act-Br), 2089320(Bz-act-I-Form 1), 2089321(Bz-act-I- Form 2), 2089322 (2act-Cl), 2089323(2act-Br), 2089325 (3act-Cl), 2089326(3act-I), 2089327(4act-Cl), 2089329 (4act-Br), 2089330 (4act-I) contain the supplementary crystallographic data for this paper. These data are provided free of charge by the joint Cambridge Crystallographic Data Centre and Fachinformationszentrum Karlsruhe Access Structures service www.ccdc.cam.ac.uk/structures

Author Contributions

A.M.A. and C.B.A. conceived and designed the experiments; A.M.A. performed the experiments; B.B.A and P.LM performed the single-crystal X-ray crystallography; A.M.A. and C.B.A. analyzed the data and wrote the paper. All authors have read and agreed to the published version of the manuscript.

Conflicts of interest

There are no conflicts to declare.

Acknowledgements

We acknowledge the NSF-MRI grant CHE-2018414, which was used to purchase a single-crystal X-ray diffractometer and associated software employed in this study. Amila M. Abeysekera acknowledges support from the Johnson Cancer Research Center at Kansas State University, and The General Sir John Kotelawala Defence University, Sri Lanka.

[1] Dey, A., Jetti, R.K.J., Boese, R., Desiraju, G.R., *CrystEngComm,* 2003, **5**, 248-252.

[2] Pfletscher, M., Hölscher, S., Wölper, C., Mezger, M., Giese, M. *Chem. Mater* , 2017, **29**, 8462-8471.

[3]Abberley, J. P., Jansze, S. M., Walker, R., Paterson, D. A., Henderson, P. A., Marcelis, A. T., Storey, J. M. D., Imrie, C. T., Liq. Cryst, 2017, **44**, 68-83

[4] McCarthy, B. G., Pearson, R. M., Lim, C. H., Sartor, S. M., Damrauer, N. H., Miyake, G. M. J. Am. Chem. Soc, 2018, **140**, 5088-5101.

[5] He, M., Li, J., Sorensen, M. L., Zhang, F., Hancock, R. R., Fong, H. H., Pozdin, V. A., Smilgies, D. M., Malliaras, G. G., *J. Am. Chem. Soc*, 2009, **131**, 11930-11938.

[6] Wang, J., Song, Y., Sun, P., An, Y., Zhang, Z., Shi, L., Langmuir, 2016, **32**, 2737-2749.

[7] Chen, L., Xiang, J., Zhao, Y., Yan, Q. *J. Am. Chem. Soc*, 2018, **140**, 7079-7082

[8] Beale, T. M., Chudzinski, M. G., Sarwar, M. G., Taylor, M. S., *Chem. Soc. Rev*, 2013, **42**, 1667-1680.

[9] Desiraju, G. R., *Angew. Chem., Int. Ed.* 2007, **46**, 8342-8356

[10] Etter, M. C., *Acc. Chem. Res.* 1990, **23**, 120−126

[11] Aakeröy, C. B., Chopade, P. D., Desper, J., *Cryst. Growth Des.*2011, **11**, 5333-5336.

[12] Aakeröy, C. B., Epa, K., Forbes, S., Schultheiss, N., Desper, J., *Chem. Eur. J,* 2013, **19**, 14998-15003.

[13] Murray, J. S., Lane, P., Clark, T., Politzer, P., *J. Mol. Model*, 2007, **13**, 1033-1038.

[14] McDowell, S. A., *Chem. Phys. Lett.* 2014, **598**, 1-4.

[15] Lim, J., Y.Beer, P. D., *Chem*. 2018, **4**, *4*731-783.

[16] Clark, T., Hennemann, M., Murray, J. S., *J. Mol. Model*. 2007, **13**, 291-296.

[17] Messina, M. T., Metrangolo, P., Panzeri, W., Ragg, E., Resnati, G., *Tetrahedron Lett*. 1998, **39**, 9069−9072.

[18] Metrangolo, P., Panzeri, W., Recupero, F., Resnati, G., J. *Fluorine Chem.* 2002, **114**, 27−33

[19] Desiraju, G. R., Harlow, R. L., J. *Am. Chem. Soc.* 1989, **111**, 6757−6764

[20] Kniep, F., Stefan H.J., Qi, Z., Sebastian M. W., Severin, S., Ingo, S., Eberhardt, H., Stefan, M. H., *Angew. Chem., Int. Ed*. 2013, **52**, 7028-7032.

[21] Lange, A., Heidrich, J., Zimmermann, M. O., Exner, T. E., Boeckler, F. M., J. *Chem. Inf. Model*. 2019, **59**, 885-894.

[22] Khavasi, H. R., Hosseini, M., Tehrani, A. A., Naderi, S., *CrystEngComm*, 2014, **16**, 4546-4553.

[23] Aakeröy, C. B., Wijethunga, T. K., Desper, J.,Daković, M., *Cryst. Growth Des*. 2015. 15, 3853-3861.

[24] Metrangolo, P., Meyer, F., Pilati, T., Resnati, G., Terraneo, G., *Angew. Chem., Int. Ed*. 2008, **47**, 6114−6127.

[25] Perkins, C., Libri, S., Adams, H., Brammer, L. *CrystEngComm* 2012, **14**, 3033−3038.

[26] Aakeröy, C. B., Baldrighi, M., Desper, J., Metrangolo, P., Resnati, G. *Chem. - Eur. J*. 2013, **19**, 16240−16247.

[27] Abeysekera, A.M., Day, V.W., Sinha, A.S., Aakeröy, C.B., *Cryst. Growth Des*. 2020, **20**, 7399–7410.

[28] Guevara-Vela, J. M., Romero-Montalvo, E., Costales, A., Pendás, Á. M., Rocha-Rinza, T. *Phys. Chem. Chem. Phys*., 2016, **18**, 26383-26390.

[29] Gilli, G., Bellucci, F., Ferretti, V., Bertolasi, V. *J. Am. Chem. Soc*,, 1989, ***111***, 1023-1028.

[30] Abeysekera, A. M., Averkiev, B. B., Sinha, A. S., Le Magueres, P., Aakeröy, C. B., *ChemPlusChem*. 2021, **86**, 1-10

[31] Politzer, P., Murray, J. S., *ChemPhysChem* 2013, **14**, 278−294.

[32] Rosokha, S. V., Neretin, I. S., Rosokha, T. Y., Hecht, J., Kochi, J. K., *Heteroat.Chem*. 2006, **17**, 449−459.

[33] Clark, T., Politzer, P., Murray, J. S., *Mol. Sci*. 2015, **5**, 169−177.

[34] Holthoff, J. M., Engelage, E., Weiss, R., Huber, S. M. *Angew. Chem., Int. Ed*., 2020, ***59***, 11150-11157.